Supergene Pb-Cu-(Sb) mineral assemblage in abandoned epithermal deposit Rudno nad Hronom, Slovakia

Jozef Vlasáč[1], Tomáš Mikuš[1], Martin Ondrejka[2], Peter Žitňan[3,4] & Peter Tuček[5]

[1] Earth Science Institute, Slovak Academy of Sciences, Ďumbierska 1, 974 01 Banská Bystrica, Slovakia; vlasac@savbb.sk, mikus@savbb.sk
[2] Department of Mineralogy, Petrology and Economic Geology, Faculty of Natural Sciences, Comenius University in Bratislava, Ilkovičova 6, 842 15 Bratislava, Slovakia; martin.ondrejka@uniba.sk
[3] Rudné Bane, Kammerhofská 7, 969 01, Banská Štiavnica, Slovakia; zitnan@rudnebane.sk
[4] Department of Geology and Palaeontology, Faculty of Natural Sciences, Comenius University in Bratislava, Ilkovičova 6, 842 15 Bratislava, Slovakia; zitnan2@uniba.sk
[5] Prospech Ltd., Križovatka 25, 969 01, Banská Štiavnica, Slovakia

AGEOS

Abstract: An unusual assemblage of Pb-Cu-(Sb)-(Mn) supergene minerals, represented by mottramite, phosphohedyphane, mimetite, minerals of the segnitite-beudantite series, anglesite, cerussite, oxyplumboroméite, brochantite, devilline, gypsum and coronadite was recently identified at the Priečna, Johan de Deo and Anna-Zubau epithermal ore veins near Rudno nad Hronom, Štiavnické vrchy Mts., Slovak Republic. Mottramite is a rare mineral at the Rudno deposit and this is the first reported occurrence in the Western Carpathians. Also phosphohedyphane occurs only rarely at the deposit. The $Pb^{2+} \leftrightarrow Ca^{2+}$ substitution between phosphohedyphane and pyromorphite was observed. An extensive substitution between As and S was recognised on the T site in the minerals of the beudantite – segnitite series. Anglesite and cerussite are relatively abundant supergene minerals, especially in the proximity of primary galena relicts. Secondary Cu sulphates (brochantite and devilline) are only secondary minerals found also in macroscopic size. Brochantite forms dark green tabular crystals up to 0.1 mm. Devilline occurs as a light green-blue acicular crystals grown on brochantite. Gypsum was found with this assemblage. Rare coronadite, Mn supergene mineral is also found at the Rudno nad Hronon locality.

Key words: Western Carpathians, Neogene Banská Štiavnica stratovolcano, mottramite, phosphohedyphane, mimetite, segnitite-beudanite, devilline, brochantite, coronadite

1. INTRODUCTION

Origin of secondary minerals is connected with hypogenous processes at ore deposits. Supergene Pb-Zn-Cu mineralisations in Western Carpathians are often subjects of mineralogical research, especially in the last two decades. From the base metal deposits or occurrences (Banská Štiavnica, Čavoj, Valaská Belá, Jasenie-Soviansko, Poniky-Drienok, Ochtiná – Mária-Margita and others) mimetite (Števko et al., 2015, 2018[a]), cerussite (e. g., Luptáková & Chovan, 2003; Števko & Bálintová, 2008; Števko et al., 2008, 2018a), pyromorphite (Števko et al., 2008, 2018[a]) and other lead secondary minerals – anglesite, wulfenite (citations above) are known. Copper secondary mineral assemblage, represented by brochantite and devilline was recently described from the Cu deposits Špania Dolina – Piesky (Števko et al., 2013) but also from the base metal deposit Poniky – Drienok and Poniky – Farbište (Števko et al., 2011, 2018[a]) as well as from the epithermal deposit Hodruša-Hámre or Banská Štiavnica (Števko and Malíková 2014; Števko et al., 2018[b]). The oxidation zone of the Rudno nad Hronom deposit is not well developed, nevertheless some interesting secondary minerals were recently recognised. The primary epithermal precious metal (Au-Ag) and base-metal mineralisation was not object of this study.

2. HISTORY OF MINING

The name of the village implies the occurrence and exploitation of precious metals, but compared to other Central-Slovakian mining towns, Rudno nad Hronom is one of the poorest in terms of production. Gold and silver mines have existed here since 1331, but the main details on mining are recorded from the late 18th century, when the old abandoned mines were reopened. However, due to low profits, most adits were closed after only three years of exploitation. Exploration works were unsuccessful and mining operated at a high deficient during the following years. As an example, in 1824 only 0.5 kg of gold and 34 kg of silver were recovered. Mining finally ceased in 1876 (Bergfest, 1953).

3. GEOLOGICAL SETTINGS

The low sulphidation epithermal mineralisation occurs in the massif of Chlm hill in hydrothermally altered andesite between Rudno nad Hronom and the village of Brehy. The deposit is formed of two groups of precious metal bearing, steeply dipping veins, striking N-S, 1-2 m thick and up to 1500 m long. The veins are intensively altered (silicification and adularisation) and the hanging-wall has developed zone of the brecciated secondary quartzites (Lexa & Smolka, 2002). The western part of the deposit is formed by the Johan de Deo, Filip, Goldschram and Priečna vein. The Anna vein structure occurs in the eastern part of the Chlm massif (Koděra et al., 1990). The structure is developed along the total length of 1500 m (Smolka et al., 1988), but only a 200 m long segment at the junction of the so-called hanging-wall golden and footwall silver branch has been the subject of exploitation. The thickness of the ore shoot reportedly reached 8–16 m; occasionally 42 m. The Au-Ag mineralisation is developed

Manuscript received 2021-02-17
Revised version accepted 2021-05-25

in the near-surface part of the veins, to of approximately 50 m depth . The vein fill is composed of quartz, carbonate and pyrite. Sulphides (galena, sphalerite, chalcopyrite and Ag-sulphosalts) are less frequent (Brlay, 1963). The depletion of relatively rich ore in sub-surface parts of the deposits forced the mines to close.

The epithermal system in Rudno nad Hronom is a part of the extensive system of veins of the Nová Baňa-Rudno-Pukanec ore field, and is localised at the south-western flank of the Banská Štiavnica andesite stratovolcano (Fig. 1). The Banská Štiavnica stratovolcano includes mainly products of volcanic activity of Badenian – Pannonian(16.5 to 10.5 Ma). The basement of the stratovolcano consists of crystalline rocks and a Mezozoic cover of the Veporic Unit and complexes of the Hronic Unit, but also Palaeogene and Lower Miocene sediments in locally (Konečný et al., 1995). This system of epithermal veins evolved in and was controlled by faults of the resurgent horst uplifted in the central part of the caldera. The associated hydrothermal activity formed an extensive epithermal system including 120 veins and veinlets, covering almost 100 km^2 (Lexa et al., 1999[a]). On the basis of structural aspects, vertical extent, spatial distribution and dominant mineral paragenesis, three types of epithermal veins were recognised (Lexa et al., 1999 [a], 1999[b], Lexa, 2001): 1) sulphide-rich base-metal veins ± Au, in the east-central part of the horst ("Štiavnica type"); 2) Ag–Au ± base-metal veins in the central-western part of the horst ("Hodruša type"); and 3) Au–Ag veins related to marginal faults of the horst ("Kremnica type"). The veins are vertical zoned with Au–Ag, upper and lower Pb–Zn, and Cu zones (Koděra, 1963).

4. METHODS

Samples for the mineralogical study were collected from the Johan de Deo adit from the Priečna and Johan de Deo veins and from the waste dumps at old workings Zubau from the Anna vein system (Fig. 1). Samples labeled RUDD-004 came from exploration diamond drill-hole RUDD-004 drilled by Prospech Ltd. The drillhole was collared at E 329043 and N 5363050 (WGS 84 UTM 34N). The targets for drill hole are Filip and Goldschram veins. Standard thin sections and polished sections of representative mineralisation were studied in transmitted and reflected light. Electron microprobe analyses (EMPA) of secondary minerals were performed on a JEOL JXA 8530FE in a wavelength-dispersive mode (WDS) at the Earth Sciences Institute of Slovak Academy of Sciences in Banská Bystrica under the following conditions: accelerating voltage 15 kV, probe current

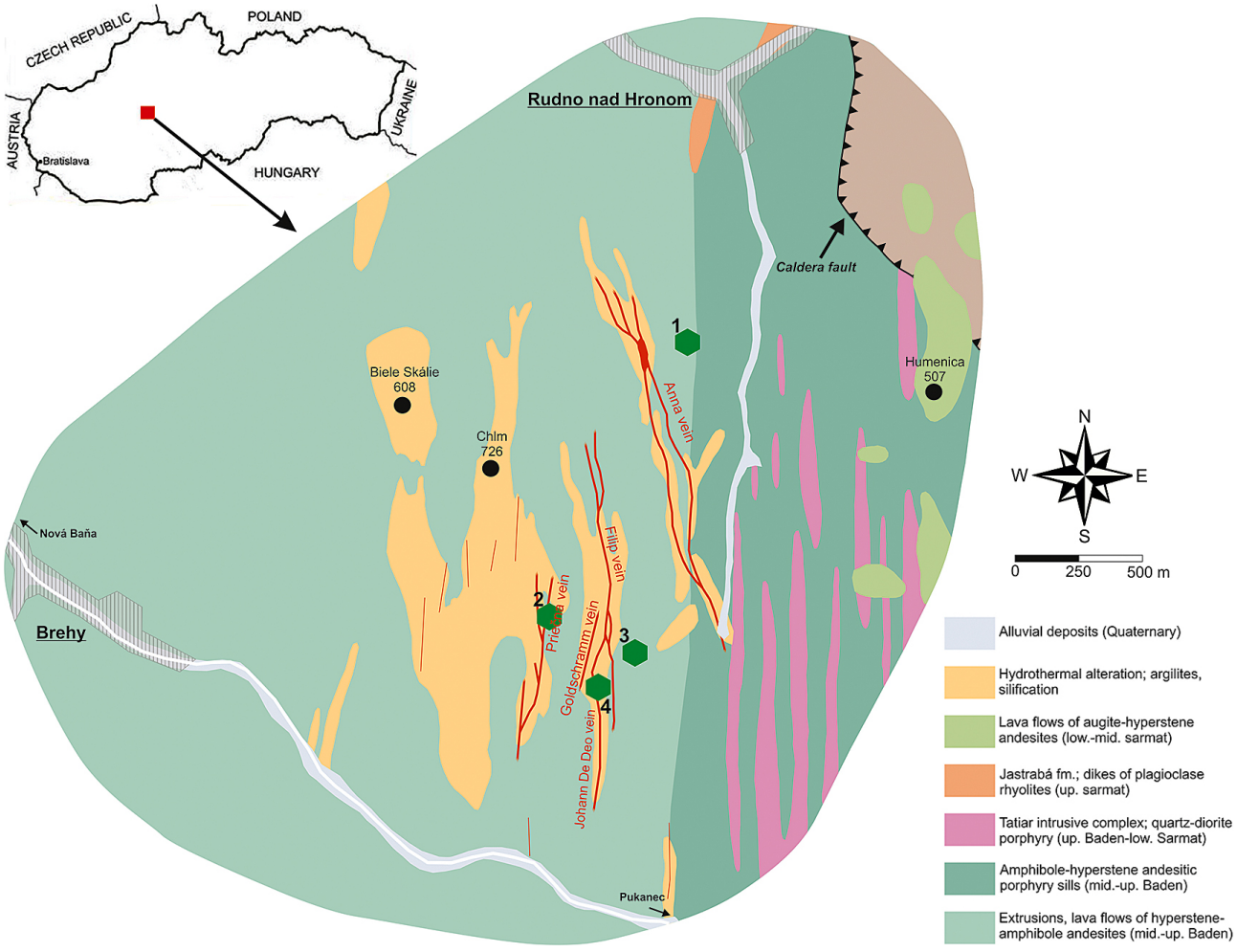

Fig. 1: Simplified geological map of the Rudno nad Hronom deposit with ore veins, adits and exploration pits after Peter Paudits (Bakos et al., 2017). "List of sample localisation: 1 - Zubau adit, tailings from the Anna vein; 2 - Priečna vein; 3 - Borehole RUDD-004; 4 - Johan De Deo vein."

15 nA, beam diameter 2-8 μm, ZAF correction, counting time 10 s on peak, 5 s on background. Following standards were used: As(Lα) - GaAs, Pb(Mβ) - crocoite, Ca(Kα) – diopside, Cu(Kα) - cuprite, Zn(Kα) – gahnite, Mn(Kα) – rhodonite, Fe(Kα) – hematite, Sb(Lα) – stibnite, Sr(Lα) – celestite, Ba(Lα) and S(Kα) – baryte, P(Kα) – apatite, Al(Kα) – corundum, Na(Kα) – albite, Si(Kα) – quartz, V(Kα) – ScVO4, Cl(Kα) – tugtupite, F(Kα) – fluorite, K(Kα) - orthoclase.

The powder X-Ray diffraction data of devilline were obtained on Bruker D8 Advance diffractometer (Earth Science Institute, Slovak Academy of Sciences in Banská Bystrica). The measurement conditions were as follows: Lynx-Eye detector using CuKα (1.5418 Å) radiation operating at 40 kV and current 40 mA. The powder patterns were collected using Bragg-Brentano geometry in the range 2–70° 2θ, with step 0.02° 2θ/1.25 s. Unoriented powder specimen was used. Position and intensities of reflections were found and refined using ZDS software (Ondruš, 1993) and unit-cell parameters were refined using the least-squares algorithm by software UnitCell (Holland & Redfern, 1997).

5. RESULTS

5.1. Mineralogy of the secondary phases

Mottramite, ideally $PbCu(VO_4)OH$ is a member of adelite-descloizite group of minerals with the general formula $AB(XO_4)(OH)$; which contains intermediate-size divalent cations (Ca and Pb) at the A site, divalent transition metals (Cu, Zn, Fe, Mn, Mg, Co and Ni) at the B site and X = P, As^{5+} or V^{5+} (Gaines et al., 1997). Mottramite occurs in thin rims (2 μm) around gold and uytenbogaardtite and it is associated with phosphohedyphane (Fig. 2a). It was rarely observed only at Priečna vein. Lead is the dominant cation at the A site ranging from 55.01 to 58.58 wt % of PbO (0.96–1.00 *apfu* Pb) and Ca rarely reaches up to

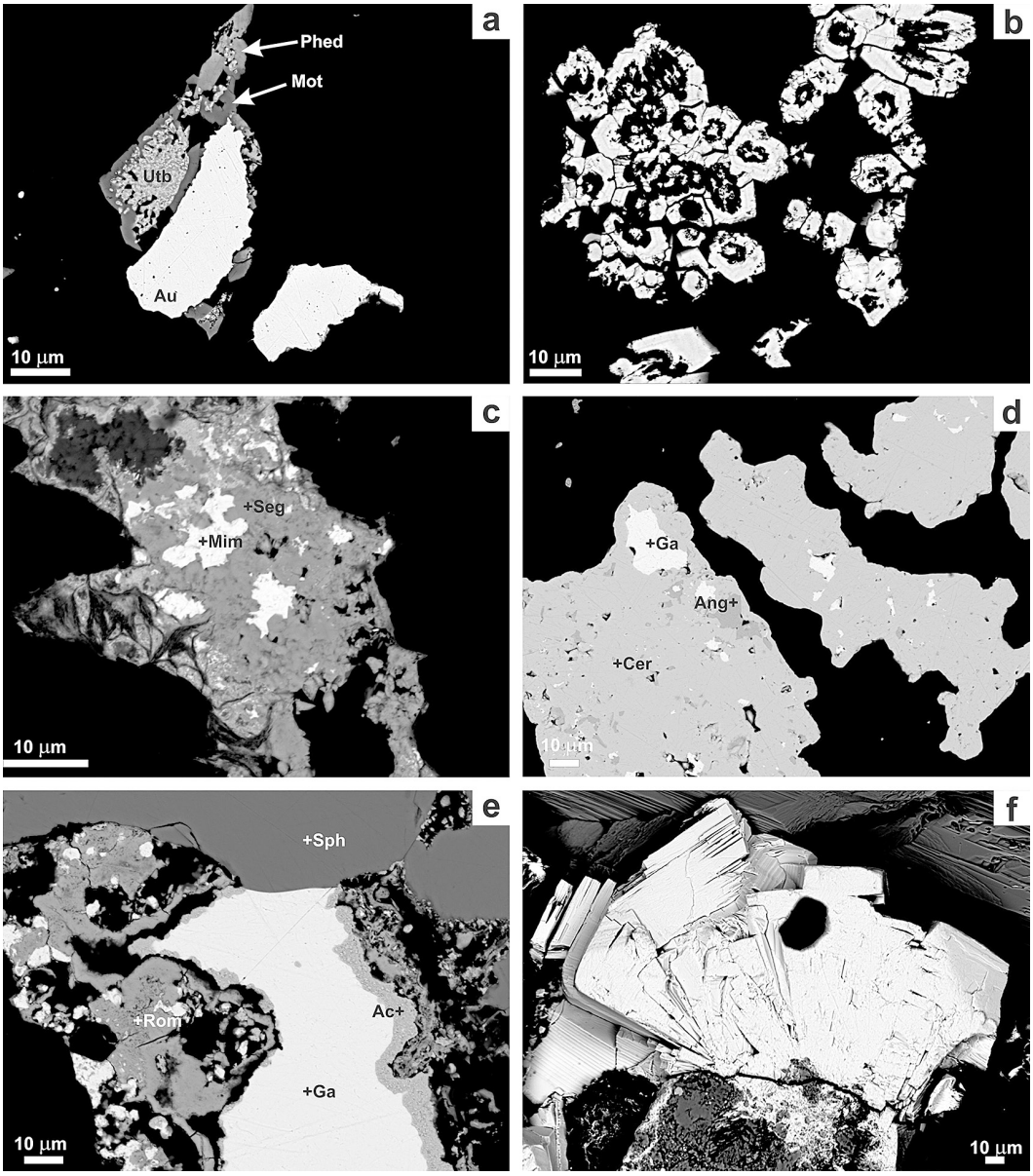

Fig. 2:
a – Thin rims of mottramite (Mot) associated with phosphohedyphane (Phed) surrounding aggregate of gold (Au) and uytenbogaardtite (Utb).
b – Zoned euhedral crystals of phosphohedyphane. Heterogeneity is the result of various Ca and Pb content.
c – Mimetite (Mim) associated with segnitite-beudantite (Seg).
d – Galenite grains (Ga) almost completely replaced by anglesite (Ang) and cerussite (Cer).
e – Oxyplumboroméite (Rom) associated with galena (Ga), sphalerite (Sph), acanthite (ac).
f – Tabular crystals of brochantite. All images are back-scattered images from the microprobe.

Tab. 1: Chemical composition of mottramite from the Rudno nad Hronom deposit. Formula is based on 3 *apfu*, H_2O content was calculated from stoichiometric constraints. General formula is $AB(TO_4)(OH)$.

sample / analyse	PR-0107							
	1	2	3	4	5	6	7	8
CaO	0.47	0.51	0.22	0.43	0.52	0.36	0.64	0.30
SrO	0.20	0.26	0.00	0.21	0.17	0.00	0.18	0.28
MnO	0.09	0.07	0.14	0.00	0.17	0.05	0.03	0.04
FeO_{total}	0.49	0.29	0.50	0.70	0.89	0.75	1.05	0.99
ZnO	1.04	1.22	0.79	0.99	0.72	0.60	0.77	0.49
CuO	17.96	17.07	18.21	17.29	17.66	16.38	16.67	16.46
PbO	56.43	56.16	55.01	56.19	56.58	58.58	57.20	57.10
SiO_2	0.15	0.37	0.30	0.25	0.08	0.51	0.55	0.40
V_2O_5	19.22	19.67	17.68	18.32	15.96	17.72	18.12	19.20
P_2O_5	2.32	2.23	2.52	2.48	2.77	3.28	2.66	2.28
As_2O_5	1.57	1.57	1.97	1.47	5.08	1.75	1.99	1.50
SO_3	0.05	0.01	1.71	0.94	0.08	0.09	0.04	0.09
H_2O_{calc}	2.31	2.30	2.32	2.35	2.33	2.28	2.30	2.27
Total	**102.29**	**101.72**	**101.37**	**101.58**	**102.99**	**102.36**	**102.20**	**101.40**
Ca^{2+}	0.03	0.04	0.02	0.03	0.04	0.03	0.04	0.02
Sr^{2+}	0.01	0.01	0.00	0.01	0.01	0.00	0.01	0.01
Mn^{2+}	0.00	0.00	0.01	0.00	0.01	0.00	0.00	0.00
Fe^{2+}	0.03	0.02	0.03	0.04	0.05	0.04	0.06	0.05
Zn^{2+}	0.05	0.06	0.04	0.05	0.03	0.03	0.04	0.02
Cu^{2+}	0.88	0.84	0.89	0.83	0.86	0.81	0.82	0.82
Pb^{2+}	0.98	0.99	0.96	0.99	0.99	1.04	1.00	1.02
∑ M	1.98	1.95	1.94	1.96	1.99	1.95	1.97	1.95
Si^{4+}	0.01	0.02	0.02	0.02	0.01	0.03	0.04	0.03
V^{5+}	0.82	0.85	0.76	0.79	0.68	0.77	0.78	0.84
P^{5+}	0.13	0.12	0.14	0.13	0.15	0.18	0.15	0.13
As^{5+}	0.05	0.05	0.07	0.05	0.17	0.06	0.07	0.05
S^{6+}	0.00	0.00	0.08	0.05	0.00	0.00	0.00	0.00
∑ T	1.02	1.05	1.06	1.06	1.01	1.05	1.03	1.05

0.64 wt % of CaO (0.04 *apfu* Ca). The B site is predominantly occupied by copper, Cu ranging from 16.38 to 18.21 wt % of CuO (0.81–0.89 *apfu* Cu). Amounts of Zn are only minor (0.49–1.22 wt % ZnO and 0.02–0.06 *apfu* Zn). Iron content is ranging from 0.29 to 1.05 w% of FeO (0.02–0.06 *apfu* Fe) (Fig. 3). Vanadium is the dominant element at the X site (up to 19.22 wt % V_2O_5; 0.85 *apfu* V^{5+}), but the systematic presence of other pentavalent

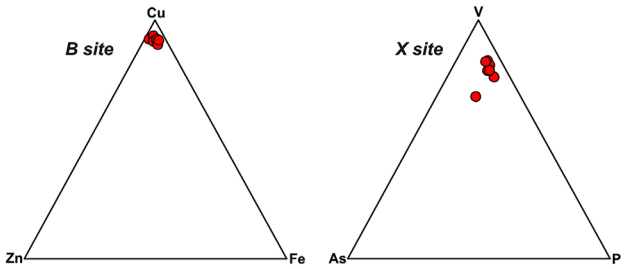

Fig. 3: Ternary plot at the B site and T site (apfu) in mottramite from the Rudno nad Hronom deposit.

cations is also documented (<3.28 wt % of P_2O_5; 0.18 *apfu* P and <5.08 wt % of As_2O_5; 0.17 *apfu* As) – (Tab. 1).

Phosphohedyphane $Ca_2Pb_3(PO_4)_3Cl$, member of the apatite supergroup is the only phosphate mineral detected in the studied samples. It occurs in the samples of Priečna vein and forms anhedral aggregates associated with uytenbogaardtite, gold and mottramite (Fig. 2a). It also occurs as euhedral prismatic crystals rarely up to 20 μm in size (Fig. 2b). Representative microprobe analyses of the phosphohedyphane are given in Table 2. The phosphohedyphane has a heterogeneous chemical composition (Fig. 4), mainly due to Ca and Pb substitution at the M site. The Pb concentration ranges from 70.97 to 77.21 wt % of PbO (3.46–4.08 *apfu* Pb) and Ca varies between 4.43 and 7.36 wt % of CaO (0.96–1.45 *apfu* Ca), which corresponds to 0.71–0.81 Pb/(Pb + Ca) atomic ratio. The two members of this solid solution with the lowest Ca content belong to the pyromorphite field in the apatite–phosphohedyphane–pyromorphite compositional area (Fig. 4). The amount of divalent cations (Cu, Zn, Sr, Ba) is low and do not exceed 0.05 *apfu*. The dominant cation at the T site is phosphorus, ranging from 15.22 to 18.71 wt % of P_2O_5 (2.57–2.9 *apfu* P), but some compositions have increased As_2O_5 (3.23 wt %, 0.34 *apfu* As). Although the X site occupancy shows that all compositions belong to the Cl-dominant member. The calculated OH^- content varies between 0.07–0.19 *apfu*.

Mimetite belongs to the pyromorphite group and was found in the Zubau old mining tailings. It forms relicts up to 10 μm corroded and replaced by segnitite (Fig. 2c). Its composition is rather simple. Lead is the dominant cation ranging from 71.71 to 74.50 wt % of PbO (4.75–4.92 *apfu* Pb). Only minor substitution with iron and Sr was observed. FeO content reaches up to 0.90 wt % (0.19 *apfu* Fe) and Sr rarely reaches 0.70 wt % SrO (0.10 *apfu* Sr). Arsenic is the dominant cation (up to 22.89 wt % of As_2O_5; 2.94 *apfu* As), and the presence of sulphur is also documented (<0.84 wt% of SO_3; 0.16 *apfu* S). The calculated

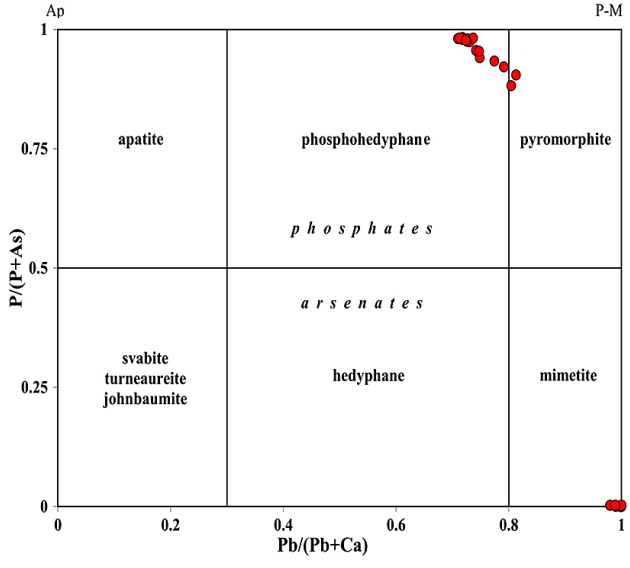

Fig. 4: Compositions of phosphohedyphane from the Rudno nad Hronom deposit in a Pb/(Pb + Ca) versus P/(P + As) classification diagram (atomic proportions).

empirical formulas of mimetite and microprobe analyses are given in (Tab. 3) and are plotted in the Fig. 4.

Segnitite and *beudantite* are the members of the alunite supergroup, which includes trigonal (rhombohedral) sulphates, phosphates, and arsenates with the general formula of $DG_3(TO_4)_2(OH)_6$, where the species-defining constituents are as follows: tetrahedrally coordinated T = S^{6+}, P^{5+}, As^{5+}; octahedrally coordinated cations G = Al^{3+},Fe^{3+}, V^{3+}, Ga^{3+}, Cu^{2+}, Zn^{2+}; and large cations D = K^+, Na^+, Tl^+, Ag^+, H_3O^+, Ca^{2+}, Sr^{2+}, Ba^{2+}, Pb^{2+}, REE^{3+}, Bi^{3+}, Th^{4+}. The ideal formula of segnitite is $PbFe^{3+}_3(AsO_4)(AsO_3OH)(OH)_6$ and beudantite has half of the T position occupied by the SO_4 anion (e. g., Jambor, 1999; Kolitsch & Pring, 2001; Bayliss et al., 2010). The members of segnitite – beudantite solid solution were found at Zubau mine tailings. They occur in association with mimetite and limonite as anhedral aggregates with size up to 50 μm usually, replacing mimetite (Fig. 2c) and limonite. Their chemical composition is quite simple, no distinct substitutions were observed. The D site is fully occupied by lead. The Pb content ranges from 32.64 to 34.79 wt % of PbO (1.00 *apfu* Pb). The G position is dominantly occupied by Fe^{3+}.The FeO content ranges from 26.04–30.09 wt % (2.59–2.89 *apfu* Fe^{3+}). The main substitution is $Fe^{3+} \leftrightarrow Al^{3+}$ (Fig. 5). Aluminum content ranges from 0.26 to 2.31 wt % of Al_2O_3

Tab. 2: Chemical composition of phosphohedyphane from the Rudno nad Hronom deposit, formula is based on 5 *apfu*. General formula is $M_5(TO_4)_3X_q$. Contents of S, F and Al are below the detection limits. n. a. – not analysed.

sample / analyse	PR-0107									
	1	2	4	5	6	11	12	22	21	22
CaO	4.65	6.88	7.34	6.85	6.27	4.43	6.19	6.36	7.01	7.24
SrO	0.00	0.00	0.00	0.00	0.00	0.23	0.00	0.00	0.00	0.16
BaO	0.22	0.04	0.00	0.08	0.11	0.15	0.17	0.01	0.00	0.00
MnO	0.07	0.10	0.00	0.06	0.01	0.02	0.06	0.05	0.00	0.05
FeO	0.16	0.37	0.05	0.00	0.20	0.07	0.14	0.10	0.16	0.07
ZnO	0.21	0.16	0.32	0.12	0.00	0.28	-	-	-	-
CuO	0.09	0.00	0.04	0.02	0.02	0.00	0.00	0.11	0.09	0.00
PbO	76.20	72.96	72.59	72.15	73.84	76.52	73.34	72.72	70.97	73.07
SiO_2	0.11	0.22	0.07	0.01	0.16	0.04	0.05	0.00	0.02	0.01
V_2O_5	0.04	0.00	0.00	0.05	0.03	0.03	0.05	0.06	0.13	0.00
P_2O_5	15.22	18.55	18.66	18.06	17.79	15.38	17.25	17.48	18.23	18.55
As_2O_5	3.23	0.60	0.53	0.73	1.35	2.58	1.72	1.28	0.50	0.62
Cl	2.76	2.97	2.83	2.88	2.93	2.46	2.89	2.83	2.86	3.02
Total	**102.96**	**102.88**	**102.44**	**101.01**	**102.73**	**102.22**	**101.86**	**101.01**	**99.96**	**102.79**
Ca^{2+}	0.96	1.34	1.42	1.36	1.25	0.92	1.25	1.28	1.40	1.40
Sr^{2+}	0.00	0.00	0.00	0.00	0.00	0.03	0.00	0.00	0.00	0.02
Ba^{2+}	0.02	0.00	0.00	0.01	0.01	0.01	0.01	0.00	0.00	0.00
Mn^{2+}	0.01	0.02	0.00	0.01	0.00	0.00	0.01	0.01	0.00	0.01
Fe^{2+}	0.03	0.06	0.01	0.00	0.03	0.01	0.02	0.01	0.02	0.01
Zn^{2+}	0.03	0.02	0.04	0.02	0.00	0.04	-	-	-	-
Cu^{2+}	0.01	0.00	0.00	0.00	0.00	0.00	0.00	0.01	0.01	0.00
Pb^{2+}	3.96	3.56	3.53	3.61	3.71	4.00	3.72	3.68	3.56	3.56
∑ M	5.02	5.00	5.00	5.01	5.01	5.01	5.01	5.00	5.00	5.00
Si^{4+}	0.02	0.04	0.01	0.00	0.03	0.01	0.01	0.00	0.00	0.00
V^{5+}	0.00	0.00	0.00	0.01	0.00	0.00	0.00	0.01	0.01	0.00
P^{5+}	2.49	2.85	2.85	2.84	2.81	2.53	2.75	2.78	2.88	2.84
As^{5+}	0.33	0.06	0.05	0.07	0.13	0.26	0.17	0.13	0.05	0.06
∑ T	3.00	3.00	3.00	3.00	3.00	3.00	3.00	3.00	3.00	3.00
OH^-_{calc}	0.10	0.09	0.13	0.09	0.07	0.19	0.08	0.10	0.10	0.07
Cl	0.90	0.91	0.87	0.91	0.93	0.81	0.92	0.90	0.90	0.93
∑ T	1.00	1.00	1.00	1.00	1.00	1.00	1.00	1.00	1.00	1.00

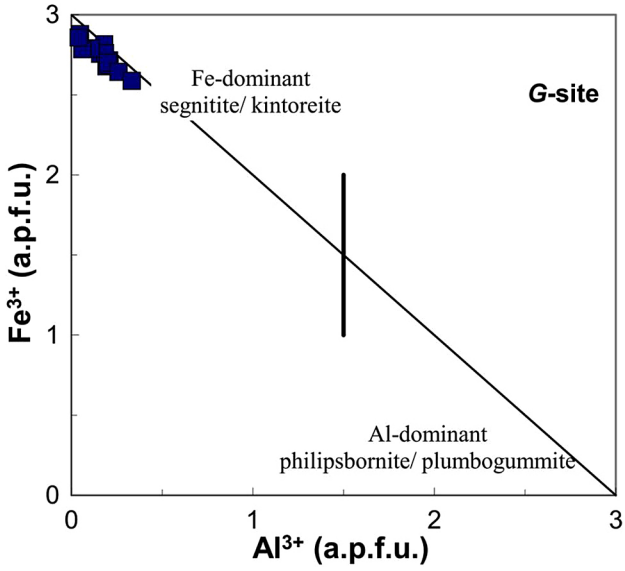

Fig. 5: Substitution on the G-site in the segnitite-beudantite solid solution from the Rudno nad Hronom deposit.

Tab. 3: Chemical composition of mimetite from the Rudno nad Hronom deposit, formula is based on 5 *apfu*. General formula is $M_5(TO_4)_3X_q$. Contents of P, Si, Ca, Ba, Zn and Mn are bellow the detection limit.

sample / analyse	ZUB-3						
	13	14	20	1	2	3	4
SrO	0.00	0.20	0.70	0.00	0.41	0.32	0.00
FeO_{total}	0.46	0.90	0.24	0.41	0.57	0.10	0.24
CuO	0.04	0.13	0.04	0.00	0.04	0.00	0.03
PbO	72.51	71.71	73.54	72.94	73.73	74.24	74.50
V_2O_5	0.02	0.02	0.01	0.05	0.04	0.01	0.04
As_2O_5	22.38	22.50	22.65	21.89	21.93	22.89	22.35
SO_3	0.63	0.84	0.07	0.62	0.75	0.62	0.59
Cl	2.24	2.35	2.46	2.27	2.33	2.32	2.31
Total	**98.51**	**98.68**	**100.04**	**98.29**	**100.10**	**100.65**	**100.22**
Sr^{2+}	0.00	0.03	0.10	0.00	0.06	0.05	0.00
Fe^{2+}	0.10	0.19	0.05	0.08	0.11	0.02	0.05
Cu^{2+}	0.01	0.02	0.01	0.00	0.01	0.00	0.01
Pb^{2+}	4.89	4.75	4.84	4.91	4.77	4.91	4.92
∑ M	5.02	5.00	5.03	5.01	5.00	5.00	5.00
V^{5+}	0.00	0.00	0.00	0.01	0.01	0.00	0.01
As^{5+}	2.93	2.90	2.89	2.86	2.76	2.94	2.87
S^{6+}	0.12	0.16	0.01	0.12	0.14	0.11	0.11
∑ T	3.00	3.00	3.00	3.00	3.00	3.00	3.00
Cl^-	0.95	0.98	1.02	0.96	0.95	0.96	0.96

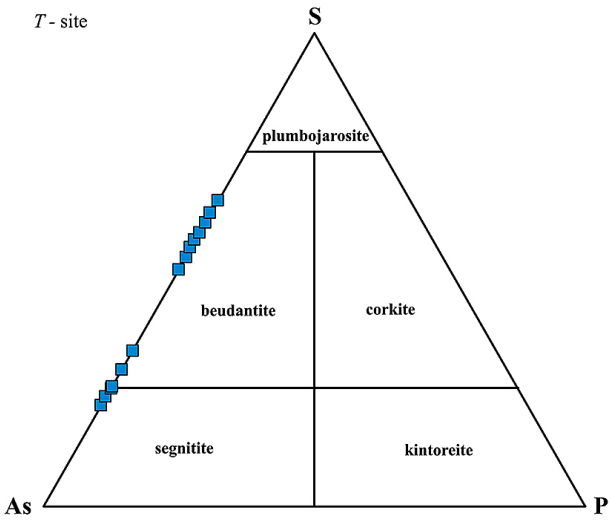

Fig. 6: Classification diagram of the part of alunite supergroup minerals with the plot of analysed points from the Rudno nad Hronom deposit.

Tab. 4: Chemical composition of segnitite-beudantite from the Rudno nad Hronom deposit, formula is based on 4 *apfu*. H_2O content was calculated from stoichiometric constraints. General formula is $DG_3(TO_4)_2(OH)_6$.

sample	ZUB-3									
analyse	7	5	4	8	6	17	18	3	11	16
SrO	0.14	0.00	0.09	0.04	0.20	0.00	0.00	0.18	0.08	0.00
BaO	0.00	0.09	0.18	0.00	0.22	0.00	0.00	0.00	0.37	0.00
ZnO	0.10	0.02	0.09	0.22	0.07	0.00	0.00	0.10	0.08	0.11
CuO	0.26	0.14	0.22	0.72	0.35	0.61	0.63	0.25	0.83	1.13
FeO	30.09	29.35	29.18	28.06	27.03	27.95	27.40	26.38	27.02	26.04
PbO	32.64	32.83	33.30	33.47	33.21	33.08	33.79	32.93	33.67	34.79
Al_2O_3	1.27	1.46	1.58	1.46	1.84	0.83	0.40	2.31	0.32	0.26
SiO_2	0.09	0.07	0.55	0.29	0.07	0.02	0.08	0.10	0.71	0.56
P_2O_5	0.04	0.03	0.01	0.00	0.03	0.00	0.03	0.00	0.05	0.06
As_2O_5	11.66	13.05	13.17	16.04	20.63	21.42	22.35	22.36	21.54	22.54
SO_3	15.02	14.01	13.09	11.08	7.74	6.35	5.73	5.40	5.37	4.52
H_2O_{calc}	8.88	8.78	8.82	8.67	8.51	8.29	8.19	8.35	8.17	8.05
Total	**100.19**	**99.82**	**100.31**	**100.08**	**99.90**	**98.57**	**98.66**	**98.44**	**98.21**	**98.06**
Sr^{2+}	0.01	0.00	0.01	0.00	0.01	0.00	0.00	0.01	0.01	0.00
Ba^{2+}	0.00	0.00	0.01	0.00	0.01	0.00	0.00	0.00	0.02	0.00
Zn^{2+}	0.01	0.00	0.01	0.02	0.01	0.00	0.00	0.01	0.01	0.01
Cu^{2+}	0.02	0.01	0.02	0.07	0.03	0.06	0.06	0.02	0.08	0.11
Fe^{2+}	2.68	2.64	2.61	2.55	2.51	2.66	2.64	2.50	2.61	2.56
Pb^{2+}	1.04	1.06	1.07	1.09	1.10	1.13	1.17	1.11	1.16	1.22
Al^{3+}	0.18	0.20	0.22	0.21	0.27	0.12	0.06	0.34	0.05	0.04
∑ M	3.93	3.92	3.94	3.94	3.94	3.98	3.93	4.00	3.94	3.94
Si^{4+}	0.01	0.01	0.07	0.04	0.01	0.00	0.01	0.01	0.09	0.07
P^{5+}	0.00	0.00	0.00	0.00	0.00	0.00	0.00	0.00	0.01	0.01
As^{5+}	0.72	0.82	0.82	1.02	1.33	1.42	1.50	1.47	1.45	1.54
S^{6+}	1.33	1.26	1.17	1.01	0.72	0.60	0.55	0.51	0.52	0.44
∑ T	2.07	2.08	2.06	2.06	2.06	2.02	2.07	2.00	2.06	2.06
OH^-_{calc}	7	7	7	7	7	7	7	7	7	7
∑ X	7	7	7	7	7	7	7	7	7	7

(0.04–0.34 *apfu* Al^{3+}). Iron is also partially substituted by Cu. Copper content ranges from 0.14 to 1.13 wt % of CuO (0.01–0.11 *apfu* Cu). The major substitution is observed at anion T position between As and S (Fig. 6). Arsenic content ranges from 11.66 to 22.54 wt % of As_2O_5 (0.69–1.57 *apfu* As). Sulphur content varies from 4.52 to 15.02 wt % of SO_3 (0.45 to 1.26 *apfu* S). Heterogeneity on the BSE images is caused by compositional variations between S and As (Fig. 7). Representative microprobe analyses with calculated empirical formulae are given in table (Tab. 4).

Anglesite $PbSO_4$ is a common phase. It was found at all studied occurrences. It always occurs together with galena, which is often intensively replaced by anglesite. It forms rims and subhedral to anhedral aggregates up to 50 μm in size. Anglesite is usually associated with cerussite (Fig. 2d). Its chemical composition is close to theoretical end member. Lead is dominant cation, its content reach up to 74.38 wt % of PbO (1.00 *apfu* Pb). Only minor contents of Sr and Fe were detected. SrO content reach up to 0.36 wt % (0.01 *apfu* Sr) and FeO content reach up to 0.71 wt % (0.03 *apfu* Fe). Sulphur content is reaching 26.83 wt % (1.00 *apfu* S). Selected microprobe analyses of anglesite are given in Tab. 5.

Cerussite $PbCO_3$ occurs quite often. It is usually associated with relicts of primary galena and anglesite, which are intensively corroded by cerussite (Fig. 2d). It forms rims and subhedral to anhedral aggregates up to 200 μm in size. Its chemical composition corresponds to theoretical end member. The cation position is almost fully occupied by lead. PbO content reaches up to 77.63 wt % (0.98 *apfu* Pb). Only minor amounts of Fe, Ba and Sr were detected. Their content is negligible and do not exceed 0.50 wt % (0.01 *apfu*). Selected microprobe analyses are given in Tab. 5.

Tab. 5: Chemical composition of anglesite and cerussite from the Rudno nad Hronom deposit. Formulas are based on 1 *apfu*.

sample	RUDD 004					
analyse	5	6	7	14	12	13
PbO	74.38	74.16	73.82	74.33	84.08	84.39
CaO	0.00	0.01	0.00	0.01	0.05	0.04
SrO	0.24	0.36	0.19	0.00	0.00	0.55
BaO	0.13	0.00	0.11	0.00	0.29	0.00
FeO	0.45	0.71	0.47	0.45	0.20	0.26
MnO	0.00	0.03	0.08	0.00	0.00	0.03
SO_3	26.26	26.26	26.83	26.82	0.00	0.00
CO_2	-	-	-	-	16.46	16.55
Total	101.46	101.58	101.48	101.60	101.08	101.83
Pb^{2+}	1.00	1.00	0.99	0.97	0.98	0.97
Ca^{2+}	0.00	0.00	0.00	0.00	0.00	0.00
Sr^{2+}	0.01	0.01	0.01	0.00	0.00	0.01
Ba^{2+}	0.00	0.00	0.00	0.00	0.01	0.00
Fe^{2+}	0.02	0.03	0.02	0.02	0.01	0.01
Mn^{2+}	0.00	0.00	0.00	0.00	0.00	0.00
total	1.03	1.04	1.02	0.99	1.00	0.99
S^{6+}	0.99	0.99	0.99	1.00	0.00	0.00
total	0.99	0.99	0.99	1.00		

Tab. 6: Chemical composition of oxyplumboroméite from the Rudno nad Hronom deposit. Formula is based on 4 *apfu*. *Sb^{3+} and H_2O were calculated from stoichiometric constraints. General formula is $A_2B_2O_6X$.

sample	PR-0715A					
analyse	41	42	43	44	45	46
Na_2O	0.11	0.12	0.13	0.06	0.12	0.05
CaO	3.73	3.71	3.68	3.55	3.69	3.62
SrO	5.22	5.22	4.98	4.88	4.69	4.41
MnO	0.06	0.11	0.14	0.16	0.07	0.09
FeO	2.65	2.65	2.85	2.75	2.26	2.54
ZnO	0.39	0.75	0.51	1.71	1.64	0.51
CuO	0.00	0.03	0.05	0.12	0.00	0.10
Ag_2O	0.53	0.09	0.35	0.57	2.37	0.82
PbO	24.50	26.08	24.59	25.42	24.29	28.62
Al_2O_3	0.20	0.16	0.18	0.16	0.12	0.25
SiO_2	3.15	3.18	3.16	3.01	2.81	3.19
As_2O_5	0.31	0.43	0.26	0.37	0.33	0.44
Sb_2O_5	58.69	59.01	57.15	57.88	56.11	56.02
$*H_2O_{calc}$	0.16	0.16	0.15	0.16	0.15	0.16
Total	**99.90**	**101.86**	**98.46**	**100.81**	**98.78**	**100.90**

sample	PR-0715A					
analyse	41	42	43	44	45	46
Na^+	0.02	0.02	0.02	0.01	0.02	0.01
Ca^{2+}	0.38	0.37	0.38	0.36	0.38	0.37
Sr^{2+}	0.29	0.29	0.28	0.27	0.26	0.24
Mn^{2+}	0.00	0.01	0.01	0.01	0.01	0.01
Fe^{2+}	0.19	0.19	0.21	0.20	0.16	0.18
Zn^{2+}	0.03	0.05	0.04	0.12	0.12	0.04
Cu^{2+}	0.00	0.00	0.00	0.01	0.00	0.01
Ag^{2+}	0.03	0.00	0.02	0.03	0.12	0.04
Pb^{2+}	0.63	0.66	0.64	0.65	0.63	0.74
$*Sb^{3+}$	0.42	0.40	0.39	0.35	0.29	0.36
Σ A	2.00	2.00	2.00	2.00	2.00	2.00
Al^{3+}	0.02	0.02	0.02	0.02	0.01	0.03
Fe^{3+}	0.00	0.00	0.00	0.00	0.00	0.00
Si^{4+}	0.30	0.30	0.31	0.28	0.27	0.30
Sb^{5+}	1.66	1.66	1.66	1.68	1.70	1.64
As^{5+}	0.02	0.02	0.01	0.02	0.02	0.02
Σ B	2.00	2.00	2.00	2.00	2.00	2.00
OH	0.02	0.02	0.02	0.02	0.02	0.02
Σ X	1.000	1.000	1.000	1.000	1.000	1.000

Oxyplumboroméite belongs to the roméite-group minerals of the pyrochlore supergroup with the general formula $A_2B_2O_6X$ where: A = Na, Ca, Ag, Mn, Sr, Ba, Fe^{2+}, Pb, Sn^{2+}, Sb^{3+}, Bi^{3+}, Y, REE, Sc, U, Th, □ (= vacancy); B = Ta, Nb, Ti, Sb^{5+}, W, V^{5+}, Sn^{4+}, Zr, Hf, Fe^{3+}, Mg, Al and Si; and X = O, OH, plus lesser substitute of F, H_2O (Atencio et al., 2010). Currently, there are five valid members of the roméite group: oxycalcioroméite – $Ca_2Sb_2O_7$ (Christy & Gatedal, 2005), oxyplumboroméite – $Pb_2Sb_2O_7$ (Christy & Gatedal, 2005), fluorcalcioroméite – $(Ca,Na)Sb_2O_6F$ (Brugger et al., 1997; Uher et al., 1998; Brugger & Gieré 1999), hydroxycalcioroméite $[(Ca,Sb^{3+})_2(Sb,Ti^{4+})_2O_6F]$ (Rouse et al., 1998; Zubkova et al., 2000) and hydroxyferroroméite - $(Fe^{2+}_{1.5}\square 0.5)Sb^{5+}_2O_6(OH)$ (Mills et al., 2017). At the Rudno nad Hronom deposit, oxyplumboroméite occurs as irregular aggregates up to 100 μm. It is associated with sphalerite and galena (Fig. 2e) and was found at Johan de Deo vein. The B position is dominantly occupied by Sb^{5+} (range from 1.64 to 1.73 *apfu*). Considerable amount of Si^{4+} was found in our oxyplumboroméite, its content is reaching up to 0.30 *apfu*. All of Si was assigned to the B position despite Atencio's et al., (2010) recommendation that for formula calculation, no more than 50 % of Si can be attributed to the B position. Due to the "oversaturation" of the B position by Sb and from the stoichiometric constraints it is concluded that some Sb was in fact Sb^{3+} on the A sites. The content of Sb^{3+} is up to 0.42 *apfu*. Pb is usually the dominant cation occupying the A position (the maximal content is 0.74 *apfu*). The A position contains also variable proportions of Ca (max. 0.38 *apfu*)

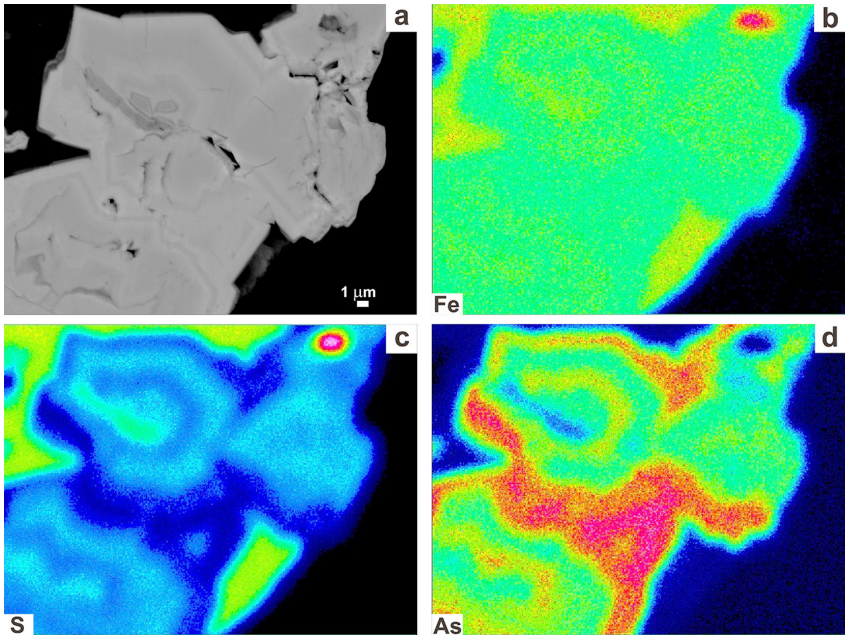

Fig. 7: Back-scattered electron image and X-ray (compositional) maps showing element distribution (Fe, S, As) in the segnitite-beudantite from the Rudno nad Hronom deposit.

Fig. 8: Assemblage of brochantite (dark green) devilline (light green-blue) and gypsum (transparent) crystals from the Priečna vein, Rudno nad Hronom deposit. The width of the the image is 8 mm.

Tab. 7: Chemical composition of brochantite from the Rudno nad Hronom deposit, formula is based on 4 *apfu*. H_2O content was calculated from stoichiometric constraints.

sample / analyse	JDD-S3					
	2	6	7	9	10	11
CaO	0.03	0.06	0.15	0.04	0.03	0.05
FeO	0.00	0.03	0.04	0.08	0.08	0.05
CuO	69.29	67.10	68.20	68.12	70.09	70.15
Al_2O_3	0.27	0.30	0.15	0.32	0.29	0.47
SiO_2	0.24	0.16	0.14	0.04	0.20	0.07
P_2O_5	0.03	0.08	0.06	0.05	0.08	0.07
SO_3	18.22	18.29	17.73	18.76	18.21	18.76
H_2O_{calc}	11.67	11.39	11.44	11.57	11.78	11.88
Total	**99.84**	**97.48**	**97.96**	**99.04**	**100.78**	**101.62**
Ca^{2+}	0.00	0.01	0.01	0.00	0.00	0.00
Fe^{2+}	0.00	0.00	0.00	0.00	0.00	0.00
Cu^{2+}	3.92	3.89	3.94	3.89	3.93	3.90
Al^{3+}	0.02	0.03	0.01	0.03	0.02	0.04
∑ M	3.95	3.93	3.97	3.93	3.97	3.95
Si^{4+}	0.02	0.01	0.01	0.00	0.01	0.01
P^{5+}	0.00	0.01	0.00	0.00	0.01	0.00
S^{6+}	1.02	1.05	1.02	1.06	1.01	1.04
∑ T	1.05	1.07	1.03	1.07	1.03	1.05

Tab. 8: Chemical composition of devilline from the Rudno nad Hronom deposit. Formula is based on 7 cations. H_2O and OH were calculated from stoichiometric constraints. n. a. – not analyzed.

sample / analyse	JDD-S1								
	7	8	9	10	5	4	3	2	1
CaO	8.09	8.29	8.08	8.60	8.34	8.78	8.13	8.06	8.89
MgO	0.00	0.01	0.01	0.00	0.00	0.00	0.01	0.00	0.03
MnO	0.00	0.13	0.09	0.10	0.20	0.16	0.11	0.01	0.05
CuO	49.23	50.68	50.03	50.24	51.77	49.36	49.49	51.18	49.11
ZnO	0.17	0.11	0.62	0.22	0.05	0.95	0.91	0.00	0.00
SO_3	25.77	25.44	26.07	24.87	24.03	24.47	24.65	24.31	24.89
As_2O_5	0.08	0.03	0.05	0.00	0.00	0.07	–	–	0.05
H_2O_{calc}	16.80	17.08	17.11	16.98	17.03	16.94	16.80	16.85	16.81
Total	**100.14**	**101.77**	**102.07**	**101.00**	**101.40**	**100.72**	**100.11**	**100.41**	**99.83**
Ca^{2+}	0.93	0.94	0.91	0.98	0.94	1.00	0.93	0.92	1.02
Mg^{2+}	0.00	0.00	0.00	0.00	0.00	0.00	0.00	0.00	0.01
Mn^{2+}	0.00	0.01	0.01	0.01	0.02	0.01	0.01	0.00	0.00
∑ A Site	0.93	0.95	0.92	0.98	0.96	1.01	0.94	0.92	1.03
Cu^{2+}	3.98	4.03	3.97	4.02	4.13	3.96	4.00	4.13	3.97
Zn^{2+}	0.01	0.01	0.05	0.02	0.00	0.07	0.07	0.00	0.00
∑ B Site	4.00	4.04	4.02	4.04	4.13	4.03	4.08	4.13	3.97
S^{6+}	2.07	2.01	2.06	1.98	1.90	1.95	1.98	1.95	2.00
As^{5+}	0.00	0.00	0.00	0.00	0.00	0.00	0.00	0.00	0.00
∑ T Site	2.08	2.01	2.06	1.98	1.90	1.95	1.98	1.95	2.00
OH^-_{calc}	6.06	6.16	6.17	6.13	6.14	6.11	6.06	6.08	6.07
H_2O	3.00	3.00	3.00	3.00	3.00	3.00	3.00	3.00	3.00

Tab. 9: Devilline PXRD data from Priečna vein, Rudno nad Hronom deposit.

h	k	l	d_{obs}	I_{obs}	d_{calc}
2	0	0	10.177	100	10.159
4	0	0	5.090	43	5.080
0	1	3	4.728	2	4.678
4	0	2	4.279	8	4.257
4	1	0	3.943	<1	3.911
0	1	5	3.536	1	3.544
-5	1	0	3.392	30	3.387
-4	1	5	3.170	3	3.187
-3	1	6	3.064	7	3.060
-6	1	1	2.992	1	3.015
5	1	3	2.871	3	2.873
-2	2	3	2.786	<1	2.781
3	2	2	2.640	2	2.647
-3	1	8	2.502	1	2.497
-8	1	3	2.380	1	2.378
3	2	5	2.246	1	2.258
2	2	6	2.218	1	2.212
-9	1	2	2.165	1	2.165
2	1	9	2.110	1	2.104
0	2	8	2.026	1	2.032
1	1	10	1.994	1	1.996
-5	2	8	1.952	<1	1.950
-3	3	4	1.881	1	1.878

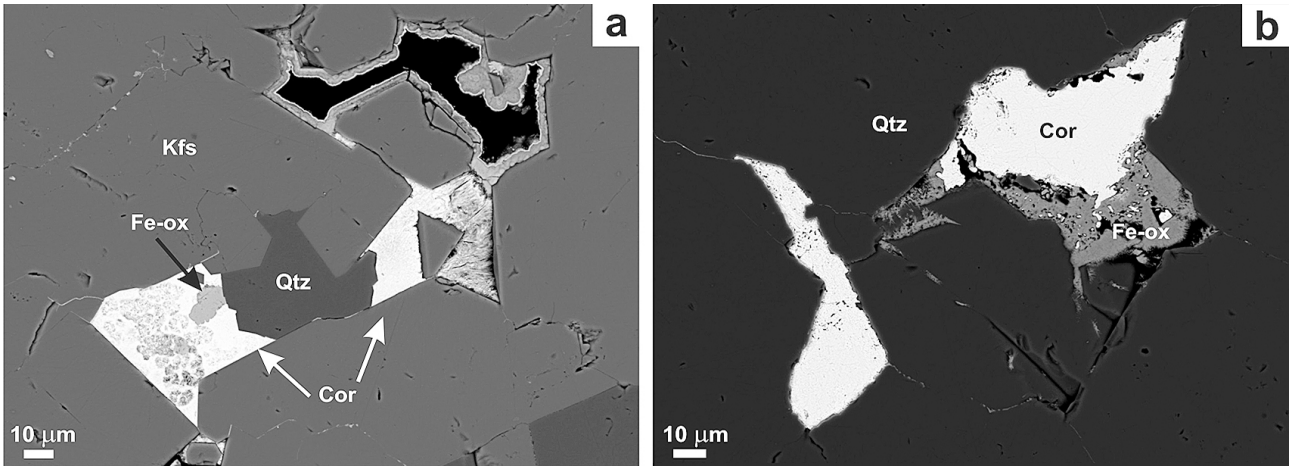

Fig. 9: a – Vugs in feldspar (Kfs) filled with coronadite (Cor). Coronadite is associated with limonite (Fe-ox). b – Vugs in quartz (Qtz) filled with coronadite (Cor). Coronadite is associated with limonite (Fe-ox). All images are back-scattered images from the microprobe.

and Sr (0.29 *apfu*). Fe (presumed ferrous) was assigned to the A position, since the assignment of Fe to the B sites results in a significant imbalance between the numbers of A and B cations. Fe content varies from 0.16 to 0.21 *apfu*. Other cations in the A position include Ag, Zn, and Na (Tab. 6). Average structural formula based on 4 cations can be expressed as $^{A}(Pb_{0.66}Ca_{0.38}Sb^{3+}_{0.37}Sr_{0.27}Fe^{2+}_{0.19}Ag_{0.04}Zn_{0.06}Na_{0.02})_{\sum 1.99}B(Sb^{5+}_{1.67}Si_{0.29}As_{0.02})_{\sum 1.98}{}^{X}(O)_{6}{}^{Y}(O_{0.98}OH_{0.02})_{\sum}1.00$.

Brochantite $Cu_4(SO_4)(OH)_6$ was found at the Priečna vein. It forms tabular crystals up to 0.1 mm with dark green color (Fig. 2f). It is associated with other sulphates; gypsum and devilline (Fig. 8). The chemical composition of brochantite corresponds to theoretical end member. Cation position is fully occupied by Cu, only minor content of Al was detected. At the anion position are slightly elevated Si and P. Representative analyses are given in Tab. 7.

Devilline $CaCu_4(SO_4)_2(OH)_6{\cdot}3(H_20)$ was found at the Priečna vein. It forms light green-blue acicular crystals up to 50 μm and occurs also as macroscopic crystalline coatings which are growing on brochantite crystals together with gypsum (Fig. 8). Its chemical composition is given in tab. 8. Zn content is low and ranges between 0 to 0.95 wt % (up to 0.07 *apfu*). It was identified also with PXRD (Tab. 9) Lattice parameters are given in the Tab. 10.

Coronadite, ideally $Pb(Mn_6^{4+},Mn_2^{3+})O_{16}$ belongs to cryptomelane group. It was found in the drill-core RUDD-004. Coronadite fills the vugs in K-feldspar (Fig. 9a) or quartz (Fig. 9b) and is associated with Fe-oxi-hydroxides (limonite?). It contains accessory amounts of Cu (up to 0.13 *apfu*), P (up to 0.04 *apfu*), Ca (up to 0.10 *apfu*), Fe (up to 0.41 *apfu*) and only minor contents of Ba, Al, Si. Microprobe analyses are given in Tab. 11.

Tab. 10: Lattice parameters calculated for the devilline from Rudno nad Hronom deposit compared with published data from other localities.

	This work	Sabelli, Zanazzi (1972)	Sejkora, Šrein (2012)	Pauliš et al. (2015)	Vrtiška et al. (2017)
a [Å]	20.826(5)	20.827(4)	20.858(5)	20.866(9)	20.872(6)
b [Å]	6.127(8)	6.131(1)	6.168(3)	6.136(2)	6.136(17)
c [Å]	22.266(96)	22.184(3)	22.09(1)	22.192(2)	22.196(9)
β [°]	102.677(96)	102.70(1)	102.71(3)	102.73(5)	102.7(4)
V [Å³]	2772.432(6)	2763(1)	2773(2)	2771(2)	2772.4(5)

6. DISCUSSION

Two principal genetic types of supergene minerals were recognised at the Rudno nad Hronom deposit. The first generation (represented by mottramite, segnitite – beudantite, phosphohedyphane, mimetite, cerussite, anglesite, oxyplumboroméite) was most likely formed in-situ and under the weathering conditions of base-metal hypogene sulphides in supergene zone. The second generation was probably formed by (sub)recent crystallization during last ≈400 years in the mine galleries. The second generation of (sub)recent supergene minerals is represented by devilline, brochantite and gypsum. Base-metal sulphides (galena, sphalerite, pyrite, minerals of the tetrahedrite group and chalcopyrite) contain metallic cations (Pb, Zn, Cu, Fe and Sb) required for crystallisation of both types of supergene minerals. The primary mineralisation was presumably rich in sulphides, e. g. pyrite, which is most probably the source of S and required for crystallization of commonly developed sulphates. The arsenates, vanadates, phosphates and carbonates are developed in a lesser extent.

The oldest notes about supergene minerals (cerussite, pyromorphite and malachite) occurrences from the Banská Štiavnica region are from the 19th century (e. g., Zipser, 1817; Zepharovich, 1859). Supergene mineral assemblage from the epithermal ore veins in the Štiavnické vrchy Mts., are subjects of several recent studies. The unusually variegated occurrence of supergene phases including azurite, baryte, cerussite, Zn-rich malachite, rosasite, smithsonite and wulfenite was identified from the subsurface parts of the Nová Anton epithermal ore vein near Hodruša-Hámre (Števko et al., 2016[a]). In addition, allophane, anglesite, brochantite, calcite, cerussite, dundasite, gypsum, hydrozincite, linarite, malachite, posnjakite and zincowoodwardite supergene mineral association was described from the abandoned Juraj adit near Hodruša-Hámre village (Števko & Malíková 2014).

Tab. 11: Chemical composition of coronadite from the Rudno nad Hronom deposit. Coronadite formula (ideally $A_{2+}(M^{4+}_6M^{3+}_2)O_{16}$ was normalized on 16 oxygen atoms. The partition of total Mn between Mn^{4+} and Mn^{3+} was calculated from neutral charge balance, . n. a. – not analysed.

sample	RUD-004-48.9						
analyse	1	2	5	6	7	8	9
Na_2O	–	–	0.04	0.09	0.03	0.10	0.20
CaO	0.59	0.41	0.36	0.33	0.34	0.34	0.51
MgO	0.12	0.00	0.00	0.00	0.00	0.00	0.04
SrO	0.03	0.18	0.07	0.05	0.11	0.02	0.01
BaO	0.74	0.09	0.07	0.12	0.00	0.05	0.26
ZnO	0.17	0.08	–	–	–	0.10	0.08
CuO	0.50	1.12	–	–	–	0.94	0.69
PbO	24.80	26.02	26.89	26.84	26.93	25.18	24.65
MnO_2	55.68	56.42	55.99	55.70	55.72	57.41	57.02
Mn_2O_3	7.93	9.41	11.71	10.91	11.72	10.51	8.68
Fe_2O_3	3.56	1.51	0.96	1.20	1.09	1.08	2.00
Al_2O_3	0.14	0.10	0.10	0.11	0.08	0.08	0.04
SiO_2	0.56	0.31	0.29	0.33	0.26	0.29	0.35
V_2O_5	–	–	0.03	0.04	0.05	0.01	–
P_2O_5	0.25	0.32	0.32	0.24	0.25	0.20	0.27
SO_3	0.09	–	0.00	0.04	0.03	0.02	0.02
Total	**95.18**	**95.98**	**96.88**	**96.04**	**96.73**	**96.41**	**94.89**
Na^+	0.00	0.00	0.01	0.03	0.01	0.03	0.06
Ca^{2+}	0.10	0.07	0.06	0.05	0.06	0.05	0.08
Mg^{2+}	0.03	0.00	0.00	0.00	0.00	0.00	0.01
Sr^{2+}	0.00	0.02	0.01	0.00	0.01	0.00	0.00
Ba^{2+}	0.04	0.01	0.00	0.01	0.00	0.00	0.02
Zn^{2+}	0.02	0.01	0.00	0.00	0.00	0.01	0.01
Cu^{2+}	0.06	0.13	0.00	0.00	0.00	0.11	0.08
Pb^{2+}	1.03	1.08	1.10	1.11	1.10	1.02	1.02
Mn^{3+}	0.96	1.14	1.41	1.33	1.42	1.26	1.05
Mn^{4+}	6.13	6.21	6.12	6.15	6.11	6.23	6.27
Fe^{3+}	0.41	0.17	0.11	0.14	0.12	0.12	0.23
Al^{3+}	0.02	0.02	0.02	0.02	0.02	0.01	0.01
Si^{4+}	0.09	0.05	0.04	0.05	0.04	0.04	0.05
V^{5+}	0.00	0.00	0.00	0.00	0.01	0.00	0.00
P^{5+}	0.03	0.04	0.04	0.03	0.03	0.03	0.04
S^{6+}	0.01	0.00	0.00	0.00	0.00	0.00	0.00
Total	**8.94**	**8.94**	**8.94**	**8.94**	**8.94**	**8.94**	**8.95**

Linarite, cerussite, rosasite, serpierite were also described from the Schöpfer vein in Hodruša-Hámre and azurite with malachite are mentioned from Rozália vein (Števko, 2015). Another mineral association of recently formed supergene minerals such are brianyoungite, brochantite, cerussite, linarite, serpierite, native sulphur and uranophane were identified at the Banská Štiavnica deposit (Števko et al., (2018[b]).

Mottramite is a relatively rare mineral and this is the first reported occurrence in the Western Carpathians. Vanadium is generally not common chemical element in epithermal systems and the source of V has not been determined but is likely to be from the Permian basement rocks. Mottramite from the epithermal systems is known to occur e. g. in the Au-Ag veins in the Carlisle mine, New Mexico, USA (McLemore, 2008). Phosphohedyphane was recently found in the Permian aplite from Veľký Zelený Potok where it is associated with cerussite and calcite and it was formed during supergene alteration of galena (Ondrejka et al., 2020).

Segnitite $PbFe_3(AsO_4)(AsO_3OH))(OH)_6$ usually forms solid solutions with philipsbornite $PbAl_3(AsO_4)(AsO_3(OH))(OH)_6$ or beudanite $PbFe^{3+}{}_3(AsO_4)(SO_4)(OH)_6$, if the substitution on the G and T sites take a place. The plumbogummite–philipsbornite and beudantite–segnitite solid solutions have been well documented (e. g., Sejkora et al., 1998, 2009; Golebiowska et al., 2016). There is significant substitution at anion position observed in segnitite-beudantite from the Rudno nad Hronom deposit. Pb–rich members of alunite supergroup from the Western Carpathians are known from several occurrences. Segnitite was reported from Rochovce-Dúbrava ore occurrence (Radková et al., 2019). Corkite and kintoreite, as products of primary sulphidic phases decomposition are known from Rainer mining field, Ľubietová-Podlipa copper deposit near Banská Bystrica (Števko et al., 2016[b]). Finally, the corkite developed by oxidation processes is known from the epithermal mineralisation Nová Baňa - Gupňa (Ferenc et al., 2014).

Among supergene Mn-oxides from the epithermal veins, todorokite has been identified at the Terézia vein in the Banská Štiavnica ore field (Háber et al., 2003) and later also coronadite (Jeleň, 2007). Coronadite and probably birnessite type compose microcrystalline collomorphous aggregates in samples from shallow parts of veins Terézia and Špitaler in the Banská Štiavnica deposit (Milovská et al., 2014). In assemblage with crystalline pyrolusite, todorokite, Zn-rich cryptomelane and chalcophanite/woodruffite were identified in the oxidation zone of hydrothermal base metal veins at Banská Štiavnica and Hodruša-Hámre (Ozdín et al., 2014). Coronadite usually can occurs as a primary mineral in hydrothermal veins or can crystallised from hot springs, but also might be of secondary origin in oxidised zones above the manganese-bearing rocks or can be found in bedded sedimentary deposits. Here, the coronadite most likely has the secondary origin due to the textural features and mineral association. The assumed secondary origin is also supported by the low totals which can suggests the low-temperature hydration. Usually, it can contain ~ 1.11 or 1.70 % of H_2O (Frondel & Heinrich, 1942; Palache et al., 1944).

7. CONCLUSIONS

Two genetic types (formed in-situ and by (sub)recent crystallization) of supergene minerals were recognised. Unusual assemblage of secondary minerals in epithermal ore veins in the Rudno nad Hronom deposit is probably formed by slightly acidic waters as a result of the reaction with pyrite and/or arsenopyrite. The oxidation of galena, tetrahedrite and chalcopytite with the acidic fluids and interaction with host rock resulted in the assemblage described in this paper.

Acknowledgements: Authors are thankful to reviewers M. Števko and S. Jeleň for critical comments which helped improve the manuscript and A. Biroň for providing PXRD data. This work was financially supported by the VEGA project (2/0028/20).

References

Atencio D., Andrade M. B., Christy A. G., Gieré R. & Kartashov P. M., 2010: The pyrochlore supergroup of minerals: nomenclature. *Canadian Mineralogist*, 48, 673–698.

Bakos F., Chovan M., Žitňan P. (Eds.), 2017: Gold in Slovakia. Lúč, Bratislava, 429 p.

Bayliss P., Kolitsch U., Nickel E. H. & Pring A., 2010: Alunite supergroup: recommended nomenclature. *Mineralogical Magazine*, 74, 5, 919–927.

Bergfest A., 1953: Rudno (pyrit): Baníctvo v Rudne nad Hronom a v Brehoch. Manuskript, Archív ŠGÚDŠ, 40 p. (in Slovak).

Brlay A., 1963: Základný ložiskový výskum na liste M-34-122-C-d Pukanec. Manuskript, Archív ŠGÚDŠ, Bratislava, 5 p. (in Slovak).

Brugger J., Gieré R., Graeser S. & Meisser N., 1997: The crystal chemistry of roméite. *Contributions to Mineralogy and Petrology*, 127, 136–146.

Brugger J. & Gieré R., 1999: As, Sb, Be and Ce enrichment in minerals from metamorphosed Fe–Mn deposit, Val Ferrera, Eastern Swiss Alps. *Canadian Mineralogist*, 37, 37–52.

Christy A. G. & Gatedal K., 2005: Extremely Pb-rich rock-forming silicates including a beryllian scapolite and associated minerals in a skarn from Långban, Värmland, Sweden. *Mineralogical Magazine*, 69, 995–1018.

Ferenc Š., Koděra P. & Demko R., 2014: Epithermal precious metals mineralization at Nová Baňa-Gupňa occurrence (Pohronský Inovec Mts., Slovak Republic). *In:* 4th CEMC, Czech Geological Society.

Frondel C. & Heinrich E. W., 1942: New data on hetaerolite, hydrohetaerolite, coronadite, and hollandite. *American Mineralogist*, 27, 48–56.

Gaines R. V., Skinner H. C. W., Foord E. E., Mason B. & Rosenzweig A., 1997: Dana's New Mineralogy. John Wiley and Sons.

Golebiowska B., Wlodek A., Pieczka A., Borkoewicz O. & Polak M., 2016: The philipsbornite–segnitite solid-solution series from Rędziny, eastern metamorphic cover of the Karkonosze granite (SW Poland). *Annales Societatis Geologorum Poloniae*, 86, 1–12.

Háber M, Jeleň S, Shkolnik E. L, Gorshkov A. A. & ZHegallo E. A., 2003: The participation of micro-organisms in the formation of todorokite from oxidation zone (Terézia vein, Banská Štiavnica deposit, Slovak Republic). Acta Miner-Petrogr, Abstract Series 1: 41

Holland T. J. B. & Redfern S. A. T., 1997: Unit cell refine-ment from powder diffraction data: the use of regression diagnostics. *Mineralogical Magazine*, 61, 65–77.

Jambor J. L., 1999: Nomenclature of the alunite supergroup. *Canadian Mineralogist*, 37, 1323–1341.

Jeleň S., 2007: Paragenetická asociácia minerálov mangánu z oxidačnej zóny žily Terézia v Banskej Štiavnici. *Mineralia Slovaca*, 39, 3, Geovestník, 21–22 (in Slovak).

Koděra M. (Ed.), 1990: Topografická mineralógia Slovenska, II. VEDA, Bratislava, 1098 p.

Koděra M., 1963: Gesetzmässigkeiten der zonalen Verteilung der Mineralisation an der subvulkanischen polymetallischen Lagerstätte Banská Štiavnica. *In*: Problems of Postmagmatic Ore Deposition 1. Geological Survey of Czechoslovakia, Prague, Czech Republic 184–189.

Kolitsch U. & Pring A., 2001: Crystal chemistry of the crandallite, beudantite and alunite groups: a review and evaluation of the suitability as storage materials for toxic metals. *Journal of Mineralogical and Petrological Sciences*, 96, 67–78.

Konečný V., Lexa J. & Hojstričová V., 1995: The Central Slovakian volcanic field: a review. *Acta Volcanologica,* 7, 63–78.

Luptáková J. & Chovan M., 2003: Supergene minerals in the Pb-Zn deposit of Jasenie-Soviansko in the Nízke Tatry Mts. *Mineralia Slovaca,* 35, 141–146 (in Slovak).

Lexa J., 2001: Metallogeny of the Banská Štiavnica stratovolcano. *Mineralia Slovaca,* 33, 203–214 (in Slovak).

Lexa J. & Smolka J., 2002: Metalogenetické hodnotenie územia SR. Manuskript, archív ŠGÚDŠ, Bratislava, 63 s. (in Slovak).

Lexa J., Štohl J. & Konečný V., 1999a : The Banská Štiavnica ore district: relationship between metallogenetic processes and the geological evolution of a stratovolcano. *Mineralium Deposita*, 34, 639–654.

Lexa J., Koděra P., Prcúch J., Veselý M. & Šály J., 1999b: Multiple stages of mineralization at the Rozália mine, Hodruša. *In:* Epithermal Mineralization of the Western Carpathians (B. T. Thompson, ed.). *Soc. Econ. Geol., Guidebook* ser. 31, 229–247.

McLemore V. T., 2008: Geochemistry and statistical analyses of epithermal veins at the Carlisle and Center mines, Steeple Rock district, New Mexico, USA, *In:* Spencer, J. E., and Titley, S. R., eds., Ores and orogenesis: Circum-Pacific tectonics, geologic evolution, and ore deposits: *Arizona Geological Society Digest* 22, p. 485–496.

Mills J. S., Christy G. A, Rumsey M., Spratt J., Bittarello E., Faveau G., Ciriotti E. M. & Berbain Ch., 2017: Hydroxyferroroméite, a new secondary weathering mineral from Oms, France. *European Journal of Mineralogy*, 29, 2, 307–314.

Milovská S., Luptáková J., Jeleň S., Biroň A, Lazor P. & Polák Ľ., 2014: Manganese oxides and oxyhydroxides from Banská Štiavnica, Ľubietová and Selce (Central Slovakia). CEMC 2014, Book of Abstracts, Skalský dvůr, 94–95.

Ondrejka M., Bačík P., Putiš M., Uher P., Mikuš T., Luptáková J., Ferenc Š. & Smirnov A., 2020: Carbonate-bearing phosphohedyphane-"hydroxylphosphohedyphane" and cerussite: supergene products of galena alteration in Permian aplite (Western Carpathians, Slovakia). *The Canadian Mineralogist,* 58, pp. 347–365.

Ondruš P., 1993: ZDS – A computer program for analysis of X-ray powder diffraction patterns. *Materials Science Forum*, 133–136, 297-300, EPDIC-2. Enchede.

Ozdín D., Kučerová G., Števko M. & Milovská S., 2014: Preliminary study of Mn-(hydro)xides in the Western Carpathians. CEMC 2014, Book of Abstracts, Skalský dvůr, 107–108.

Palache C. H., Berman & Frondel C., 1944: Dana's system of mineralogy, (7th edition), v. I, 742–743.

Pauliš P., Vrtiška L., Sejkora J., Malíková R., Hloušek J., Dvořák Z., Gramblička R., Pour O. & Ludvík J., 2015: Supergene mineralization of the skarn tin deposit Zlatý Kopec in the Krušné hory Mts. (Czech Republic). Bull mineral. -petrolog. Odd. Nár. Muz. (Praha) 23, 2, 182–200 (in Czech with English abstract).

Radková P., Mikuš T., Bakos F., Koděra P. & Luptáková J., 2019: A new type of carbonate-hosted Au mineralization at Dúbrava near Rochovce, Western Carpathians. *Acta Geologica Slovaca*, 11, 2, 103–118.

Rouse R. C., Dunn, P. J., Peacor D. R. & Wang Liping , 1998: Structural studies of the natural antimonian pyrochlores. I. Mixed valency, cation site splitting, and symmetry reduction in lewisite. *Journal of Solid State Chemistry,* 141, 562–569.

Sabelli C., Zananzzi P. F., 1972: The crystal structure of devilline. *Acta Cryst*. B, 28, 1182–1189.

Sejkora J., Čejka J., Šrein V., Novotná M. & Ederová J., 1998: Minerals of plumbogummite–philipsbornite series from Moldava deposit, Krušné

hory Mts., Czech Republic. *Neues Jahrbuch für Mineralogie, Monatshefte*, 4, 145–163.

Sejkora J., Škovíra J., Čejka J. & Plášil J., 2009: Cu-rich members of the beudantite–segnitite series from Krupka ore district, the Krušné hory Mountains, Czech Republic. *Journal of Geosciences*, 54, 355–371.

Sejkora J. & Šrein V., 2012: Supergene Cu mineralization from the Měděník hill near Měděnec, Krušné hory Mountains (Czech Republic). *Bull. Mineral. Petrolog.* Odd. Nár. Muz. (Praha) 20, 2, 255–269 (in Czech with English abstract).

Smolka J., Skaviniak M., Valko P., Kámen M., Daubner J., Petr K., Gwerk E., Novák P., Kováč P., Ružiaková B. & Mjartanová H., 1988: Záverečná správa úlohy Rudno-Brehy-Pukanec. Manuskript, Archív ŠGÚDŠ, Bratislava, 108 s.

Števko M. & Bálintová T., 2008: New findings of secondary minerals on base metals deposit Mária-Margita near Ochtiná. *Minerál*, 3, 244–248. (in Slovak)

Števko M., Ozdín D., Bačík P., Pršek J. & Gramblička R., 2008: Secondary minerals from the base metals mineralization near Valaská Belá, Slovak Republic. *Bull. mineral. -petrolog. Odd. Nár. Muz. (Praha)* 16, 2, 177–184. (in Slovak).

Števko M., Ozdín D. & Sejkora J., 2013: Supergene minerals of the Špania Dolina ore district. *Minerál* 21, 26–44 (in Slovak).

Števko M. & Malíková R., 2014: Supergene minerals from the Juraj adit, Hodruša-Hámre (Slovak Republic). *Bull. mineral. -petrolog. Odd. Nár. Muz. (Praha)* 22, 2, 261–268. (in Slovak).

Števko M., 2015: Nové nálezy na žilách v Hodruši-Hámroch. *Minerál,* 23, 5, 422–434 (in Slovak).

Števko M., Gramblička R. & Malíková R., 2015: New data on supergene minerals from the Čavoj base metal deposit, Strážovské vrchy Mts. (Slovak Republic). *Bull. mineral. -petrolog. Odd. Nár. Muz. (Praha)* 23, 1, 63–74.

Števko M., Tuček P., Sejkora J. & Malíková R., 2016a: Supergene minerals from the Nová Anton vein, Hodruša-Hámre, Štiavnické vrchy Mts. (Slovak Republic). *Bull. mineral. -petrolog. Odd. Nár. Muz. (Praha)* 24, 2, 183–193. (in Slovak).

Števko M., Sejkora J. & Malíková R., 2016b: New data on supergene minerals from the Rainer mining field, Ľubietová - Podlipa deposit (Slovak Republic). *Bull. mineral. -petrolog. Odd. Nár. Muz. (Praha)*, 24, 1, 1–12p (in Slovak).

Števko M., Sejkora J. & Súľovec Š., 2018a: New data on adelite and olivenite group minerals from Drienok deposit near Poniky, Slovakia. *In:* 5th Central-European Mineralogical Conference, Banská Štiavnica.

Števko M., Sejkora J. & Malíková R., 2018b: New data on supergene minerals from the Banská Štiavnica deposit (Slovak Republic). *Bull. Mineral. Petrolog.*, 26, 1, 90–101. (in Slovak).

Vrtiška L., Pauliš P., Gramblička R., Sejkora J., Malíková R. & Pour O., 2017: Supergene mineralization of the Michalovy Hory ore district (Czech Republic). *Bull. Mineral. Petrolog.*, 25, 2, 228–244 (in Czech with English abstract).

Uher P., Černý P., Chapman R., Határ J. & Miko O., 1998: Evolution of Nb,Ta-oxide minerals in the Prašivá granitic pegmatites, Slovakia. II. External hydrothermal Pb,Sb overprint. *Canadian Mineralogist* 36, 535–545.

Zepharovich V., 1859: Mineralogisches Lexicon für das Kaiserthum Österreich. Band I. 1-627, Wilhelm Braumüller, Wien

Zipser CH. A., 1817: Versuch eines topograhisch-mineralogischen Handbuches von Ungern. 1–440, Carl Friedrich Wigand, Oedenburg

Zubkova N. V., Pushcharovsky D. Yu., Atencio D., Arakcheeva A. V. & Matioli P. A. (2000): The crystal structure of lewisite, $(Ca,Sb^{3+},Fe^{3+},Al,Na,Mn,\square)_2(Sb^{5+},Ti)_2O_6(OH)$. *Journal of Alloys and Compounds* 296, 75–79.